Int. J. Electrochem. Sci., 17 **(2022)** Article Number: 22065, doi: 10.20964/2022.06.01

International Journal of
ELECTROCHEMICAL
SCIENCE
www.electrochemsci.org

Short Communication

First principles study of the passivity breakdown of γ–Al_2O_3 film induced by Cl^- adsorption

Xin Wei, Rou Bao, Lin Wang[*]*, Maolin Sha*

Universities Joint Key Laboratory of photoelectric detection Science and Technology in Anhui Province, Hefei Normal University, Hefei, 230601,China
[*]E-mail: wanglinhfnu@126.com

Received: 4 January 2021 / *Accepted:* 7 March 2022 / *Published:* 7 May 2022

The passivity breakdown of an anodic oxide film grown on Al was investigated by first principles calculations. Adsorption and permeation were performed to describe the reaction processes between Cl^- and surface atoms, including the structural relaxations, energies and electronic band structures. The passivity breakdown can be attributed to the thinning and collapse of film caused by the dissolution of chlorides formed by the adsorption of Cl^- instead of a permeation process. The band gap of the passive film narrows on account of the adsorption of Cl^-, which increases the electric conductivity and degrades the corrosion resistance. A mechanism model was proposed to explain the passivity breakdown, which specified the pitting initiation of Al alloys at the atomic scale. The study overcame difficulties in the experimental measurements and can be generalized to other passivity metals.

Keywords: First principles calculation; passivity breakdown; adsorption; permeation

1. INTRODUCTION

Al alloys, as structural metallic materials, have been widely applied in many fields [1-4] such as the construction industry and aerospace projects. The anodic oxide film grown on an Al surface consists of three parts: (i) an ultrathin Al_xO_y interface layer, (ii) a middle layer of γ–Al_2O_3 and (iii) a hydroxylated AlOOH terminal layer [5]. The film protects the substrate from the external environment, which is responsible for the corrosion resistance [6].

The interaction between Cl^- and the film can give rise to passivity breakdown, resulting in the eventual failure of structural components. Earlier studies indicated that the adsorption of Cl^- is the first step of pitting initiation [7-10]. The adsorption of Cl^- was first observed by the isotopic tracer method, and Berzin's work [11] illustrated that the adsorption of Cl^- was highly localized. The adsorption of Cl^- has been demonstrated by numerous studies [12-15], while the migration of Cl^- from solution to interior film is still controversial, especially regarding whether Cl^- can transfer to the interface between the film

and substrate. First principles calculations have been demonstrated to be an effective way to study the interaction between Cl^- and anodic oxide films by surface analysis techniques and electrochemical measurements in our previous study [16]. The results demonstrated that the thinning of the passive film was ascribed to the adsorption of Cl^- rather than a permeation process. Studies on the interaction between Cl^- and passive film grown on Ni were performed systematically using first principles calculations by the research group of Marcus [17-20]. It was demonstrated that the adsorption energy was positive and increased with increasing Cl^- coverage, and the permeation energy was also positive but decreased with increasing Cl^- coverage. The electrostatic interaction among ions on the surface controls the process of the reaction; in other words, electrostatic repulsion inhibits adsorption but promotes permeation. In addition, hydroxylated NiO surface-containing steps were constructed to further study the interaction between Cl^- and the surface [19]. The results indicated that both adsorption and permeation were promoted by step structures, which was much closer to the real surface state.

In this study, the adsorption and permeation of Cl^- on passive films were investigated by first principles calculations. The structural optimizations, thermodynamic energies, charge transfer and band structures were calculated. A corrosion mechanism model was built, which is appropriate for local corrosion induced by Cl^- adsorption.

2. COMPUTATIONAL DETAILS

All calculations in this study were performed by density functional theory according to the projected augmented wave method [21, 22], as performed by PWmat [23, 24]. The exchange-correlation function based on the generalized gradient approximation [25] with the Perdew–Burke–Ernzerhof functional was used. A six-layer (2×1) γ–Al_2O_3 (010) structure with a 15 Å vacuum region was adopted for the calculations of structural relaxations and electronic band structures. The upper four layers and adsorbates were allowed to relax, and the bottom two layers were fixed. van der Waals interactions were added through a forcefield [26]. The plane-wave energy cutoff was set as 520 eV, and k-point meshes were 3×4×1. The total force of each ion was decreased to less than 0.01 eV $Å^{-1}$. The configuration of the optimized structures was processed by VESTA [27].

3. RESULTS AND DISCUSSION

3.1 Adsorption of H_2O on the γ–Al_2O_3(010) surface

The adsorption of H_2O molecules on the γ–Al_2O_3(010) surface was studied to construct a hydroxylated surface to simulate the solution environment. The structural parameters and charge transfer are described in Table 1. We first investigated the adsorption of a single H_2O molecule on the surface. As shown in Fig. 1a, H_2O molecules bonded with the Al atom of the surface with a distance of 1.93 Å, which is smaller than the sum of their ionic radii, indicating chemical adsorption. The charge transfer from the surface to the H_2O molecule is 0.023 e, and the adsorption energy is -1.63 eV. The coadsorption of two H_2O molecules located at adjacent positions was considered, as shown in Fig. 1b. One of the two H_2O molecules adsorbed on the surface in molecular form, and the other H_2O molecule dissociated into OH and H, which bonded with the Al and O atoms of the surface, respectively. Both molecular and

dissociated H_2O are adsorbed on the surface through a chemical form by analyzing the bond lengths of Al-O shown in Table 1. The adsorption energy is -1.73 eV lower than that of a single H_2O molecule; that is, the interaction between H_2O molecules promotes adsorption. The charge transfer from the surface to molecular and dissociated H_2O are 0.051 and 0.121e, respectively. A small charge was found to be transferred from the surface Al to the adsorbed H_2O molecule to form aluminum hydrates, which was agreement with previous study [28], which illustrates that obtaining enough electrons is an essential condition for the dissociation of H_2O molecules.

Table 1. The bond lengths of adsorbed structures and charge transfer from surface to adsorbates.

Adsorbates	Distance/Å						Charge transfer	
	Al-O_w	Al-O_h	H-O_w		H-O_h	H-O_s	H_2O	OH+H
(H_2O-Al_{fs})	1.93	--	0.98	1.03	--	--	0.023	---
(H_2O-Al_{fs})+ (Al_{fs}-O_hH)+(O_sH)	1.99	1.73	0.98	1.09		0.98	0.051	0.121
(HO_h-Al_{fs})+(O_sH)	---	1.73	---	---	0.97	0.98	---	0.132
[(HO_h)$_2$-Al_{fs}]+2(O_sH)	---	1.76	---	---	0.98	1.01	---	0.154
[(HO_h)$_3$-Al_{fs}]+3(O_sH)	---	1.76	---	---	0.97	1.09	---	0.138
2(HO_h- Al_{fs})+2(O_sH)	---	1.73	---	---	0.97	0.98	---	0.084
3(HO_h- Al_{fs})+3(O_sH)	---	1.73	---	---	0.97	0.98	---	0.085
4(HO_h- Al_{fs})+4(O_sH)	---	1.74	---	---	0.97	0.98	---	0.104
5(HO_h-Al_{fs})+3(H_2O-Al_{fs})+5(O_sH)	1.95	1.84	0.99	1.04	0.97	1.01	0.061	0.117

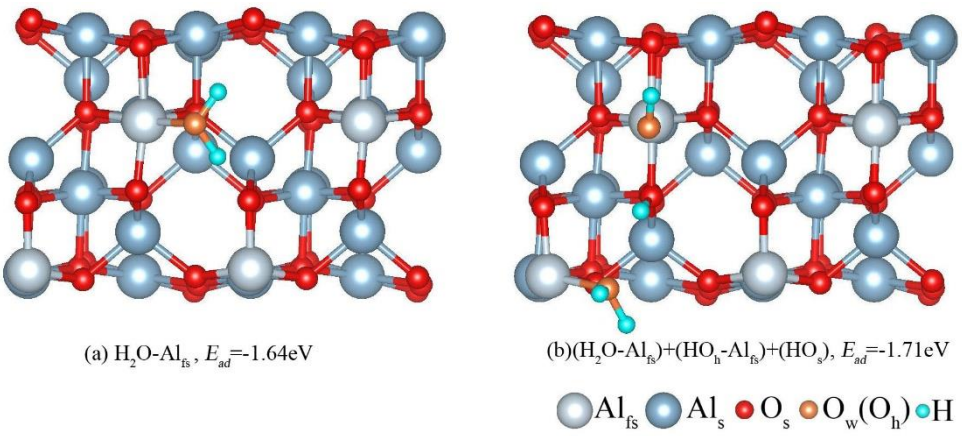

Figure 1. The adsorbed structures of H_2O molecules on the γ–Al_2O_3(010) surface: (a) single and (b) double H_2O molecules at adjacent positions.

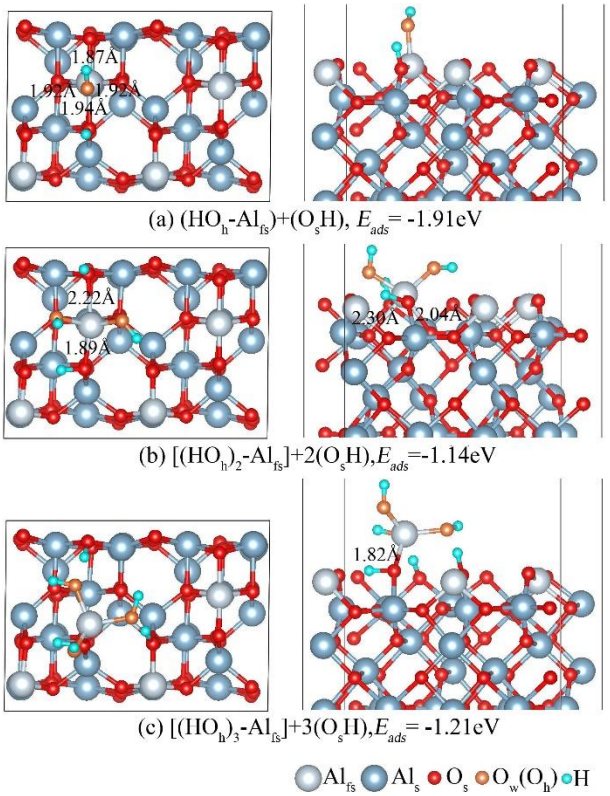

Figure 2. The adsorbed structures of dissociated H_2O on the γ–Al_2O_3(010) surface at coverages of (a) 1/2, (b) 1 and (c) 3/2 ML.

We also examined the adsorption of dissociated H_2O molecules at the same top site of Al atoms on the surface at coverages of 1/2, 1 and 3/2 ML. For single (OH+H) adsorption (Fig. 2a), OH interacted with the Al atom, and H interacted with the nearby O atom, which did not cause obvious surface reconstruction. With the coverage increasing to 1 ML, two groups of (OH+H) were placed on the surface. The two OH adsorbed on the same top site of the Al atom, and two H atoms bonded with different O atoms (Fig. 2b). The Al atom bonded with OH was pulled out of the surface along with the elongation of Al-O bonds. The Al atoms further tended to stay away from the surface when the coverage increased to 3/2 ML (Fig. 2c). The adsorption energies of dissociated H_2O (OH+H) on the surface are -1.91, -1.14 and -1.21 eV, which illustrates that H_2O molecules tend to adsorb on the surface uniformly instead of being distributed in a concentrated manner. Thus, the dissociated H_2O equally adsorbed on the surface was investigated. OH and H started to combine to form H_2O molecules, reaching a saturated state when the coverage exceeded 4 ML. The hydroxylated γ–Al_2O_3(010) surface was constructed with a (OH+H) coverage of 4 ML in this study.

3.2 Adsorption and permeation of Cl^- on hydroxylated γ–Al_2O_3(010) surface

The adsorption and permeation of Cl atoms on the hydroxylated γ–Al_2O_3(010) surface were explored to illustrate the reaction processes between Cl^- and the surface. The structures after adsorption and corresponding energies are depicted in Fig. 3. Cl^- reacted with the hydroxylated surface by the substitution of OH^-. With increasing Cl^- coverage, the surface relaxation and reconstruction became

more pronounced. The hydroxyl group of the surface can be classified into two species: (i) OH_w from dissociated H_2O molecules and (ii) OH_s generated by the binding of H atoms from H_2O molecules and O atoms from the surface. Cl^- prefers to substitute OH^- from dissociated H_2O molecules from the point of structure, which corresponds to a coverage less than 4 ML, causing very slight changes in the surface structure. The OHs started to substitute by Cl atoms along with more obvious surface reconstruction when the coverage was larger than 4 ML. Al atoms were gradually pulled out of the surface and bonded with Cl^- to produce chloride, which can dissolve in solution. This was an exothermic reaction in which each substituted energy was negative over the whole range of coverage according to Equation (1). The change in energies should be ascribed to the electrostatic interactions among ions on the surface. The substitutional energy shows an upward trend with increasing Cl coverage, indicating that their adsorption effect decreases continuously. The result agrees well with the work of Zhang et al. [29]. The adsorbed Cl^- may permeate into the interior surface by exchanging positions with O atoms in the role of electrostatic repulsion. The inserted structures and corresponding energies are shown in Fig. 4. The interior Al atoms were pulled out of the surface to participate in the formation of chloride. The permeation processes were endothermic reactions based on the definition of Equation (2), which was not a spontaneous reaction. The results are in agreement with previous studies by Bouzoubaa [20], who found that the permeation of Cl^- into the subsurface layers of oxide was an endothermic process, becoming less endothermic with increasing Cl^- coverage. Boxley et al. [30] verified that the oxide dissolution rate is related to the surface concentration of Cl^-. The experimental results of Serna et al. [31] performed by the anodic polarization method revealed that pit nucleation was related to the distribution of Cl^- and oxide modification. Thus, the change in the composition and structure of the passive film induced by adsorption and permeation affects its electrochemical behavior, which is discussed in this study.

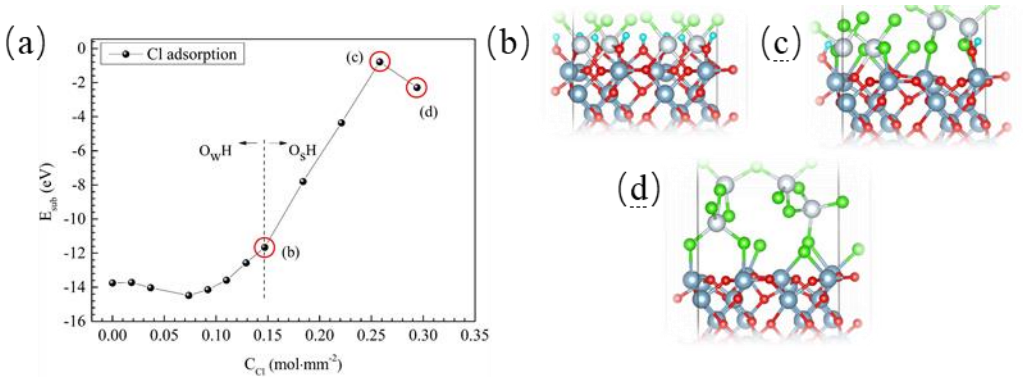

Figure 3. The substitutional energies of OH^- by Cl^- with increasing concentration of Cl atoms on the surface.

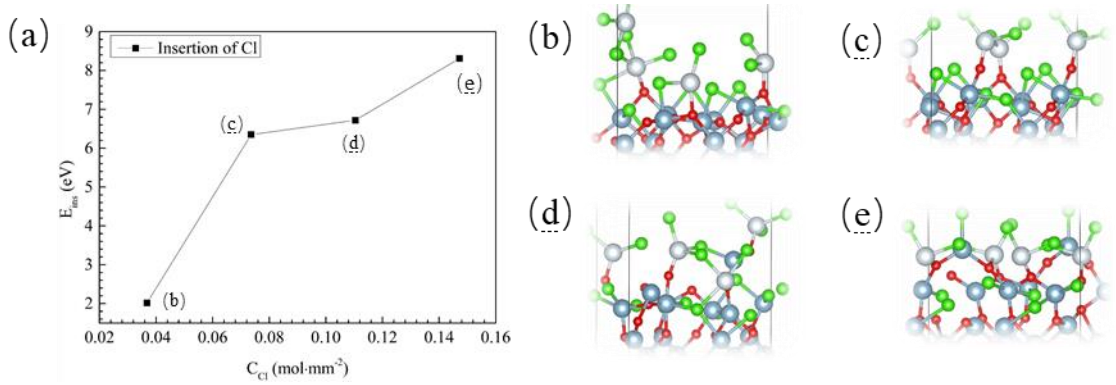

Figure 4. The insertion energies of Cl^- from the surface to the subsurface with increasing concentrations of Cl^-.

3.3 Electronic band structures

The corrosion resistance of passive films is closely related to their electronic properties [32]. The semiconductor performance of passive films can be described by electronic band structures, which are applied to estimate the electric conductivity. Generally, a film grown on a substrate has good corrosion resistance with a low electrical conductivity.

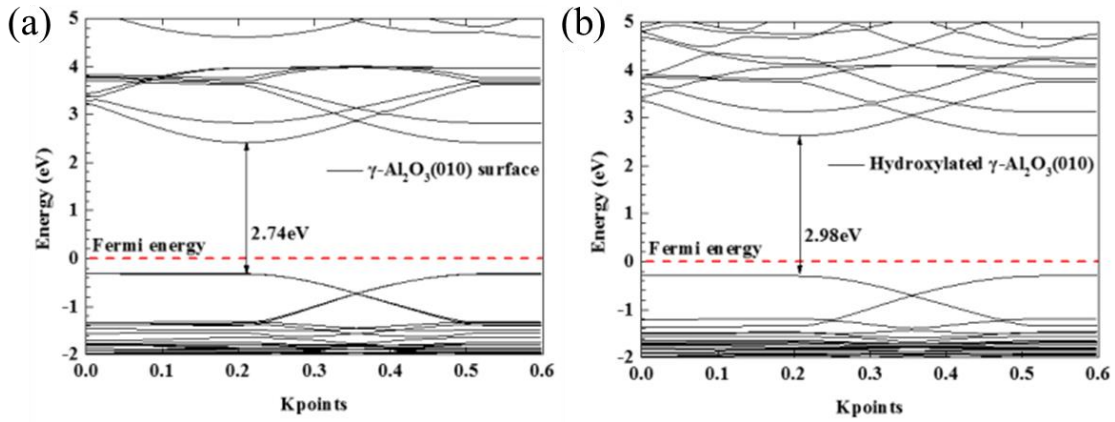

Figure 5. Electronic band structures of the (a) pristine and (b) hydroxylated γ–Al_2O_3(010) surfaces.

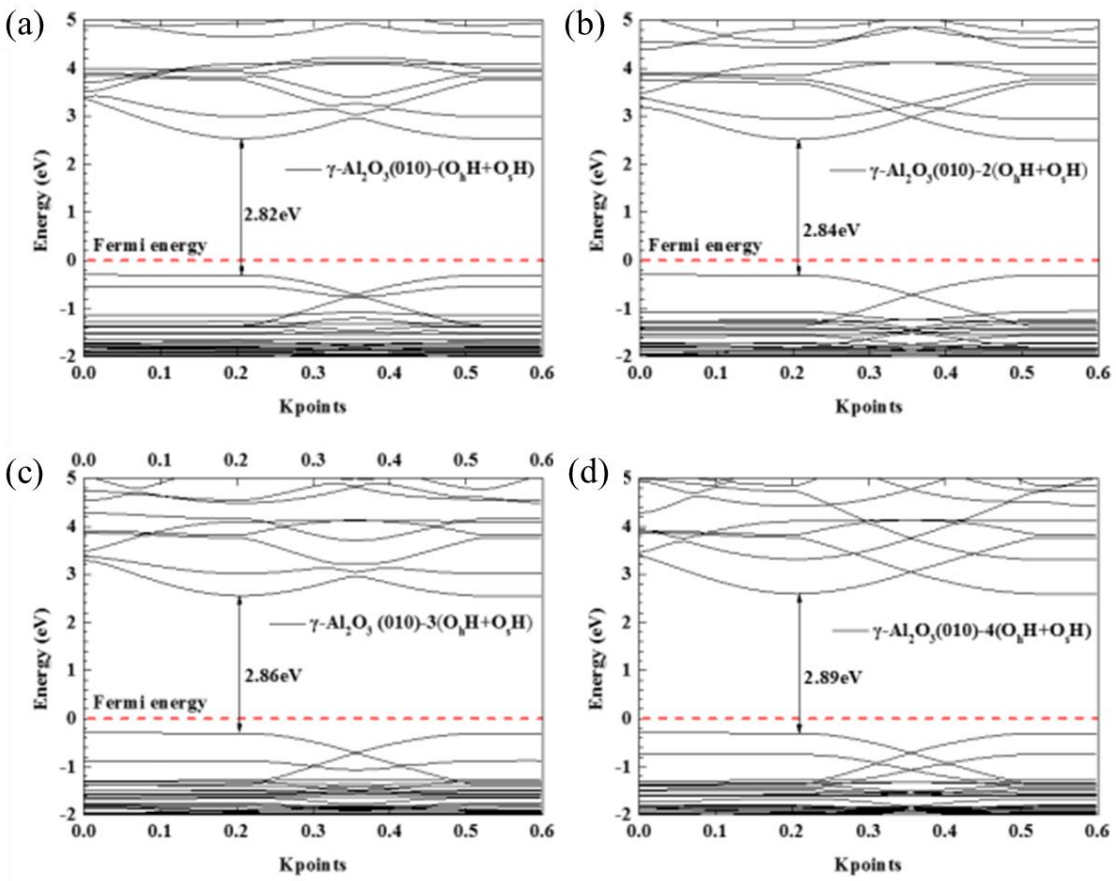

Figure 6. Electronic band structures of γ–Al_2O_3(010) surface-adsorbed dissociated H_2O molecules with coverage of (a) 1/2 ML, (b) 1 ML, (c) 3/2 ML and (4) 2 ML.

The band gap of the pristine γ–Al_2O_3(010) surface is 2.74 eV, which increases to 2.98 eV after full hydroxylation, as presented in Fig. 5. To determine the effect of the hydroxylated processes on the electric conductivity of the film, the band structures of surface-adsorbed dissociated H_2O were calculated as shown in Fig. 6. The band gap increased from 2.82 to 2.89 eV with increasing coverage from 1/2 to 2 ML, which can be explained by the hydroxylated process inducing a thickening of the film and causing a decline in electric conductivity.

As mentioned above, Cl^- tends to adsorb on the surface instead of permeating into the interior surface from the point of thermodynamic energy. As shown in Fig. 7, the band structures of γ–Al_2O_3(010) surfaces that adsorbed Cl^- were investigated. The band gap is 2.96 eV at a coverage of 2 ML, which is basically in agreement with fully hydroxylated structures. The formed chlorides are still covered on the surface and have almost no impact on the structure. The band gap gradually decreased with increasing Cl^- coverage until full chlorination was reached, which can be attributed to the dissolution of chlorides and the resulting film thinning and surface reconstruction. According to our previous studies [15], the band gap of the passive film narrows with the introduction of chloride into the electrolyte, corresponding to an increase in electric conductivity. The diffusion coefficient of vacancies increases 2-3 orders of magnitude due to the insertion of Cl, representing an increase in the transport

rate of the passive film, and has an inverse relationship with the corrosion resistance [16]. Thus, the adsorption of Cl^- leads to an increase in electric conductivity and a degradation of corrosion resistance.

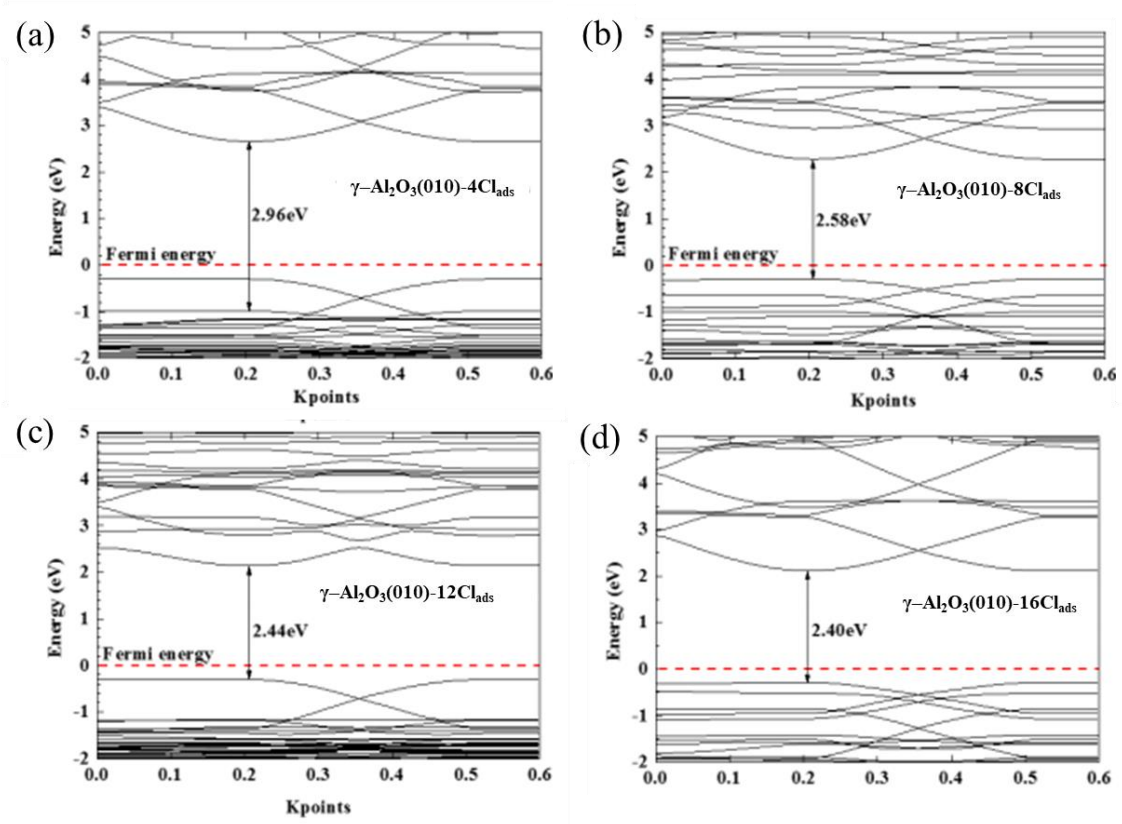

Figure 7. Electronic band structures of γ–Al_2O_3(010) surface-adsorbed dissociated H_2O molecules with coverage of (a) 2 ML, (b) 4 ML, (c) 6 ML and (4) 8 ML.

3.4 Description of the pitting corrosion mechanism

The study investigated the interaction between Cl^- and the hydroxylated γ–Al_2O_3(010) surface to reveal the mechanism of passivity breakdown for Al alloys. Adsorption can occur with a large enough driving force to guarantee a rapid reaction process, while the permeation of Cl^- cannot take place spontaneously from the point of thermodynamic energy. The hydroxylated surface forms by the adsorption of hydroxyl groups when the specimen is placed in the solution, as shown in Fig. 8(a). The chlorides formed by the adsorption of Cl^- gradually dissolved in the solution, which can cause the differential concentration of metal ions between the surface and interior. (Fig. 8(b)). The metal ions diffused from the interface to the surface to compensate for this loss, resulting in the formation and growth of voiding at the interface between the passive film and substrate (Fig. 8(c)). The passive film gradually thins with the development of interfacial voiding, which finally causes a collapse (Fig. 8(d)). The statement of this mechanism of passivity breakdown agrees with the point defect model [33-35],

which considers that the aggregation of cation vacancies at the interface between the metal and barrier gives rise to the breakdown of the passive film.

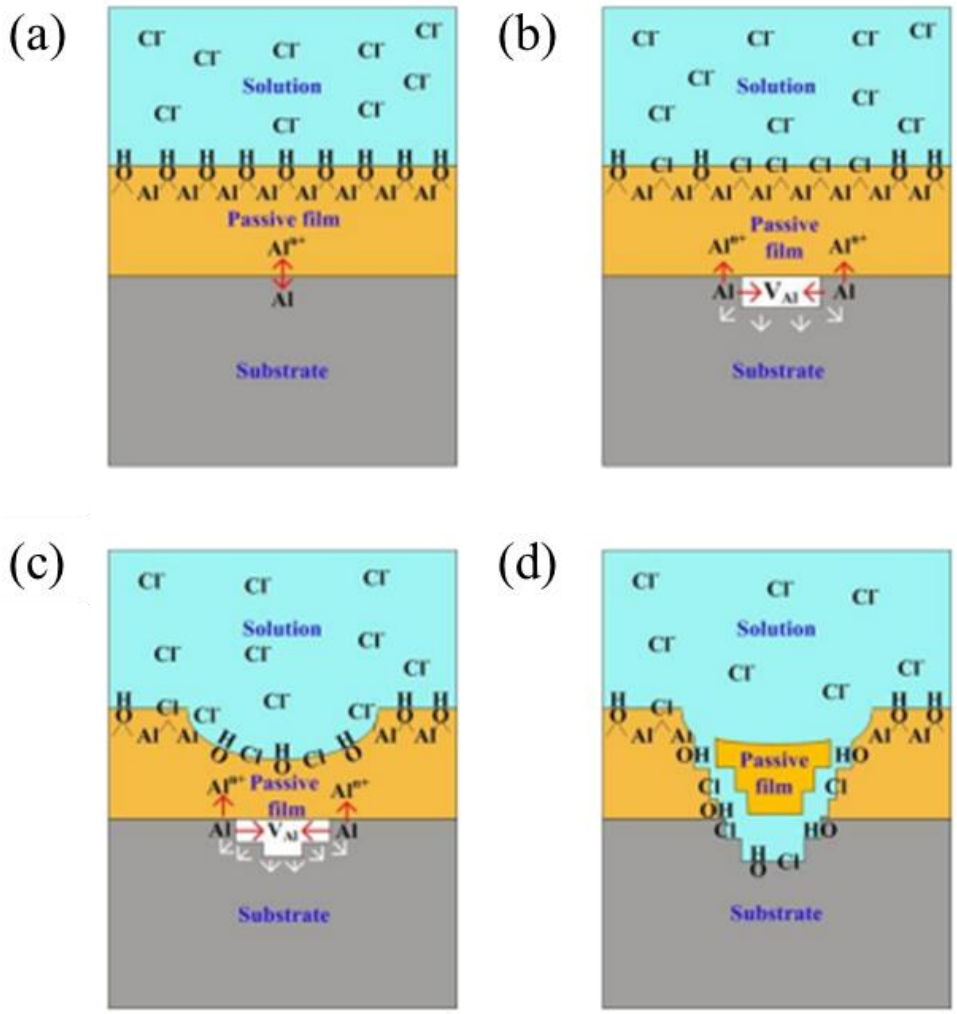

Figure 8. The schematic mechanism of passivity breakdown for the film grown on Al alloys in the solution containing Cl^-.

4. CONCLUSIONS

The adsorption and permeation of Cl^- on a γ–Al_2O_3(010) surface were performed by first principles calculations based on DFT. A hydroxylated surface was constructed to simulate the state of a passive film immersed in solution. Cl^- prefers to adsorb on the surface rather than permeate into the interior according to the adsorption energies. The formation of chlorides leads to a decline in the band gap of the passive film, which leads to a decrease in electric conductivity as well as a degradation of corrosion resistance. The study reveals that the passivity breakdown of Al alloys can be ascribed to the migration of metal ions from the interface to the solution, which agrees well with the PDM model.

ACKNOWLEDGEMENTS
This work is supported by the Natural Science Foundation of Anhui Higher Education Institution of China (KJ2019A0736), the Open Project of Key Laboratory of Structure and Functional Regulation of Hybrid Materials (Anhui University), Ministry of Education in 2020: DFT study of storage and transport of alkali metal (Li/Na/Mg) ions on layered 2D InSe surface (No.8), Hefei Normal University High-Level Talent Reaearch Startup Fund Project (2020rcjj08), the Universities Joint Key Laboratory of photoelectric detection Science and Technology in Anhui Province of China (Hefei Normal University) (2019GDTCZD03), Shanghai Changken Test Equipment Co.,Ltd: the study on electronic properties of two-dimensional semiconductor materials, and Natural Science Foundation of Anhui Province of China (1908085MB50).

References

1. A. Abu Seman, J.K.Chan, M.A Norazman, Z. Hussain, D. Brij, A. Ismail, *Anti-Corros. Method.* M., 67(2020)7.
2. N.Q. Chinh, P. Szommer, J. Gubicza , M. El-Tahawy, E.V. Bobruk, M.Y. Murashkin, R.Z. Valiev, *Adv. Eng. Mater*., 22(2020)1900672.
3. A. Albedah, B.B. Bouiadjra, , S.M.A.K. Mohammed, F. Benyahia, *Int. J. Min. Met. Mater*., 27(2020) 83.
4. Y. Zhou, P. Zhang, J. Xiong, F. Yan, *Anti-Corros. Method. M*., 66(2019)879.
5. D. Costa, T. Ribeiro, F. Mercuri, G. Pacchioni, P. Marcus, *Adv. Mater. Interfaces*, 1(2014)1300072.
6. P. Druska, H.H. Strehblow, S. Golledge, *Corros. Sci*., 38(1996)835.
7. E. McCafferty ,*Corros. Sci*., 45(2003)1421.
8. T P. Hoar,*Corros. Sci*., 7(1967)341.
9. R.T. Foley, *Corrosion*, 42(1986)277.
10. P. M.Natishan, E. McCafferty, G.K. Hubler, *J. Electrochem. Soc*., 135(1988)321.
11. A. Berzins, R.T. Lowson, K.J. Mirams, *Aust. J. Chem*., 30(1977)1891.
12. M. Liu, Y. Jin, C. Leygraf,. J. Pan, *J. Electrochem. Soc*., 166(2019)C3124.
13. P. M. Natishan, W. E O'Grady, *J. Electrochem. Soc*., 161(2014) C421.
14. M. Liu, Y. Jin, C. Zhang, C. Leygraf, L. Wen, *Appl. Surf. Sci*., 357(2015)2028.
15. A. Xu, C. Dong, X. Wei, X. Li,. D.D.Macdonald, *RSC Adv*., 9(2019)15772.
16. X. Wei., C. Dong, P. Yi, A. Xu, Z. Chen, X. Li, *Corros. Sci*., 136(2018)119.
17. N. Pineau, C. Minot, V. Maurice, P Marcus, *Electrochem. Solid St*., 6(2003)B47.
18. A. Bouzoubaa, B. Diawara, V. Maurice, C. Minotb P. Marcus, *Corros. Sci*., 51(2009)941.
19. A. Bouzoubaa, B. Diawara, V. Maurice, C. Minotb, P. Marcus, *Corros. Sci*., 51(2009)2174.
20. A. Bouzoubaa, D. Costa, B. Diawara, N. Audiffren P. Marcus, *Corros. Sci*., 2010, 52(2010)2643.
21. P.E. Blochl, *Phys. Rev*. B, 50(1994)17953.
22. G. Kresse, D. Joubert, *Physical Review B: Condensed Matter and Materials Physics*, 59(1999)1758.
23. W, Jia, J. Fu, Z. Cao, L. Wang, X. Chi, W. Gao, L. Wang., J. Comput. Phys. 251 (2013) 102
24. W, Jia, Z. Cao, L. Wang, J. Fu, X. Chi, W. Gao, L. Wang., Comput. Phys. Commun., 184 (2013) 9.
25. J.P. Perdew, K. Burke, M. Ernzerhof, *Phys. Rev. Lett.,* 77(1996)3865.
26. S.Grimme, J. Antony, S. Ehrlich, H. Krieg, *J. Chem.l Phys*., 132(2010)154104.
27. K. Momma, F. Izumi, *J. Appl. Crystallogr*., 44(2011)1272.
28. C. Zhang, B. Chen, Y. Jin, D. Sun, *J. Phys. Chem. Solids*, 110(2017)129.
29. C. Zhang, B.Chen, Y. Jin, *J. Theor. Comput Chem*. 17(2018)1850002.
30. C.J.Boxley, J.J. Watkins, H.S. White, *Solid State Lett.,* 6(2003) B38.
31. L.M. Serna, C.M. Johnson, F.D. Wall, J.C. Barbour, *J. Electrochem Soc*, 152(2005) B244.
32. Y. M Zeng,.J.L. Luo, *Electrochim. Acta*, 48(2011)3551.

33. D.D. Macdonald, A. Sun, *Electrochim. Acta*, 51(2006)1767.
34. D. D.Macdonald, *Electrochim. Acta*, 56(2011)1761.
35. E. Sikora, D.D. Macdonald, *Electrochim. Acta*, 48(2002)69-77.